2019 IEEE 30th Annual International Symposium on Personal, Indoor and Mobile Radio Communications (PIMRC): Track 1: Fundamentals and PHY

Circular Space-Time Block Code Design for Ultra-Reliable Index Modulation Schemes

Zehra Yigit[†], Ertugrul Basar[*], and Ibrahim Altunbas[†]
[†]Istanbul Technical University, Faculty of Electrical and Electronics Engineering, Maslak, 34469, Istanbul, Turkey
[*]CoreLab, Department of Electrical and Electronics Engineering, Koç University, Sariyer, 34450, Istanbul, Turkey.
E-mail: yigitz@itu.edu.tr, ebasar@ku.edu.tr, ibraltunbas@itu.edu.tr

***Abstract*—In this paper, a novel circular space-time block coding (CSTBC)-based index modulation (IM) technique, which achieves various orders of transmit diversity gains, is introduced. In the proposed system, a promising IM concept, media-based modulation (MBM), which carries additional information bits through the available radio frequency (RF) mirrors of transmit antennas, is considered. Unlike traditional STBC-based IM concepts, the proposed technique provides various orders of transmit diversity gains and attains higher spectral efficiency values with a single RF chain. The bit error rate (BER) performance of the proposed system is theoretically analyzed and an upper bound expression for the average bit error probability (ABEP) is derived. Moreover, via comprehensive computer simulations, the improved BER performance of the proposed CSTBC-IM is demonstrated over the-state-of-the-art IM schemes.**

***Index Terms*—Index modulation (IM), space-time block codes/coding (STBC), ultra-reliable communication.**

I. Introduction

To deal with stringent requirements of today's and upcoming wireless technologies, three different use cases have been defined: enhanced mobile broadband (eMBB), massive machine-type communication (mMTC) and ultra-reliable low-latency communication (URLLC) [1]. In 5G and beyond technologies, mMTC will enable an effective wireless connectivity for massive number of machine-type devices with ultra low-latency, at the sub-second level [2], which exceeds the capabilities of today's technologies. On the other hand, eMBB aims to achieve high spectral efficiency values with high reliability. Likewise, URLLC applications should achieve high reliability with low-latency constraints, which are two conflicting parameters rendering URLLC one of the key challenges in 5G and beyond technologies.

From a physical layer perspective, a reliable communication is achieved by data replication or retransmission mechanisms, where channel coding and space-time block coding (STBC) applications are considered as key enablers of ultra-reliable communication systems [3].

This work was supported by the Scientific and Technological Research Council of Turkey (TÜBİTAK) under grant no 117E869.

In the last decade, to improve the reliability and, at the same time, to attain higher spectral efficiency values, novel transmission techniques have been proposed in the context of index modulation (IM) schemes [4], which use the building blocks of the corresponding transmission systems to convey additional information bits. In the past few years, numerous studies have been carried out over broad research fields concerning spatial modulation (SM) [5] and SM-based transmission schemes. SM transmits additional information bits through the indices of the transmit antennas and has been regarded as the pioneer of the IM schemes.

Recently, a novel IM scheme called media-based modulation (MBM), which employs radio frequency (RF) mirrors in a clever manner to convey extra information bits, is introduced [6]. In the MBM scheme, a number of RF mirrors enclose the transmit antennas, and ON/OFF status of those RF mirrors create different channel state realizations for the corresponding transmit antenna. Though MBM is a recent concept, the researchers have shown a growing interest. MBM-based massive and multi-user transmission systems [7]–[9], MBM-aided secrecy communication systems [10], [11], and an STBC-based MBM technique [12], which increases the reliability of the MBM scheme through achieving a second order transmit diversity gain, are among the prominent MBM techniques. For a more detailed overview, the readers are referred to [13] and [14] and references there in.

In this study, a novel MBM-based circular STBC (CSTBC) technique, *circular space-time block coded index modulation (CSTBC-IM)*, which achieves numerous orders of transmit diversity gains, is proposed as an ultra-reliable IM concept. In the proposed CSTBC-IM scheme, the MBM concept is considered for both multiple-input-multiple-output (MIMO) and single-input-multiple-output (SIMO) system configurations. Moreover, the theoretical error performance analysis of the proposed CSTBC-IM schemes is performed and an upper bound expression is obtained for average bit error probability (ABEP). Through extensive

978-1-5386-8110-7/19/$31.00 ©2019 IEEE

computer simulations, the flexibility of the CSTBC-IM schemes that provide various orders of transmit diversity gains and achieve high spectral efficiency values, are discussed. Furthermore, their superior error performance over the reference IM techniques, such as space-time channel modulation (STCM) [12], STBC-SM [15], space-time quadrature SM (ST-QSM), uncoded space-time labeling diversity-based STCM (USTLD-STCM) [16] and classical Alamouti's STBC [17], is shown.

The rest of the paper is organized as follows. In Section II, the system models of the proposed CSTBC-IM schemes are introduced. The analytical error performance analysis is given in Section III. In Section IV, the numerical results are discussed and the paper is concluded in Section V.

II. Circular Space-Time Code Design

In the last decade, several STBC-based IM schemes [12], [15], [18], which are inspired by traditional STBC concepts [19], have been designed to provide a second order transmit diversity gain for plain IM schemes. In this study, a novel STBC technique is designed considering the structure of a circulant matrix in which each row contains the same elements as those of the first row and is determined by the circular shift of the previous row.

Suppose that $\mathbf{C}$ is a circulant matrix with dimensions $T \times P$, and it is formed by the elements c_i, for $i \in \{1, 2, \dots, P\}$, as follows:

$$\mathbf{C} = \begin{bmatrix} c_1 & c_2 & \cdots & c_T & \cdots & c_{P-1} & c_P \\ c_P & c_1 & \cdots & c_{T-1} & \cdots & c_{P-2} & c_{P-1} \\ \vdots & \ddots & \ddots & \ddots & \ddots & \ddots & \vdots \\ c_{P-T+2} & \cdots & c_P & c_1 & \cdots & c_{P-T} & c_{P-T+1} \end{bmatrix}. \quad (1)$$

Let $\mathbf{C}$ be an STBC transmission matrix and T denotes the number of time intervals. Then, when the rank criterion [19], one of the most common STBC design principles, is considered to maximize the transmit diversity, for $\mathbf{C}$ and $\hat{\mathbf{C}}$ respectively symbolizing the transmitted and erroneously detected circular STBC matrices, the transmit diversity gain is calculated by [19]:

$$G_d = \min_{\mathbf{C}, \hat{\mathbf{C}}} \operatorname{rank}\left(\left(\mathbf{C} - \hat{\mathbf{C}}\right)\left(\mathbf{C} - \hat{\mathbf{C}}\right)^{\mathrm{H}}\right) \quad (2)$$

where $(\cdot)^{\mathrm{H}}$ is Hermitian transposition. According to our exhaustive numerical tests, we reveal that when the circular $\mathbf{C}$ matrix is sufficiently sparse with a single non-zero element in each row whose position is determined by circularly shifting the previous row by one unit, it is possible to obtain a Tth order transmit diversity gain, if the following row/column ratio is satisfied:

$$r = \frac{T}{P} \leq 0.5. \quad (3)$$

Based on (1), this allows us to design transmission schemes that are highly flexible and achieve numerous orders of transmit diversity gains.

In our proposed design, we assume that s is the single non-zero element in each row of the circular STBC matrix $\mathbf{C}$, which stands for an M-ary phase shift keying/quadrature amplitude modulation (M-PSK/QAM) symbol. Moreover, the $r \leq 0.5$ is satisfied to obtain a transmit diversity order $G_d = T$.

Since the circular STBC concept requires a sparse matrix with a single non-zero element in each row or column, IM schemes are the most suitable systems to be adapted. Therefore, we combine the recent MBM transmission schemes [6], [13] with the circular STBC concept and propose a family of MBM-based CSTBC-IM schemes, including CSTBC-SM, CSTBC-MIMO, CSTBC-SIMO and CSTBC space-shift keying (CSTBC-SSK) schemes, which will be introduced in the subsequent subsections.

In general, in the proposed CSTBC-IM schemes, the transmission is performed in T time intervals and a system configuration with T_x transmit and R_x receive antennas is considered. Moreover, each transmit antenna is assumed to be surrounded by M_{rf} RF mirrors that create $P = 2^{M_{rf}}$ channel state realizations for each of those T_x antennas, where for each setup, $r \leq 0.5$ is ensured. Then, for each CSTBC-IM scheme, the incoming information bits determine the transmission vector of the first time slot, where it contains only one non-zero entry as in classical IM schemes [4]. Then, to construct the overall transmission matrix, the remaining time intervals follow the structure of a circular matrix (1).

A. CSTBC-SIMO and CSTBC-SSK

In this subsection, the CSTBC-SIMO and CSTBC-SSK transmission schemes are proposed, where the circular STBC concept is combined with the SIMO-MBM [6] transmission scheme to attain a Tth order transmit diversity gain. In the CSTBC-SIMO scheme, one transmit antenna ($T_x = 1$) with M_{rf} RF mirrors is considered, where the incoming M_{rf} bits select the index of the effective channel state out of $P = 2^{M_{rf}}$ channel state realizations and $\log_2 M$ bits determine a modulated symbol from M-PSK/QAM constellation to transmit through this selected channel state. Therefore, the spectral efficiency of the CSTBC-SIMO scheme in bits per channel use (bpcu) is given by

$$\eta_{SIMO} = \frac{M_{rf} + \log_2 M}{T} \quad \text{[bpcu]}. \quad (4)$$

In the CSTBC-SIMO scheme, the incoming ηT information bits determine the transmission vector of the first time interval, then, the overall transmission matrix is constructed by circular shifting of this transmission vector. For s being the M-PSK/QAM symbol and l being the index of the selected channel state of the

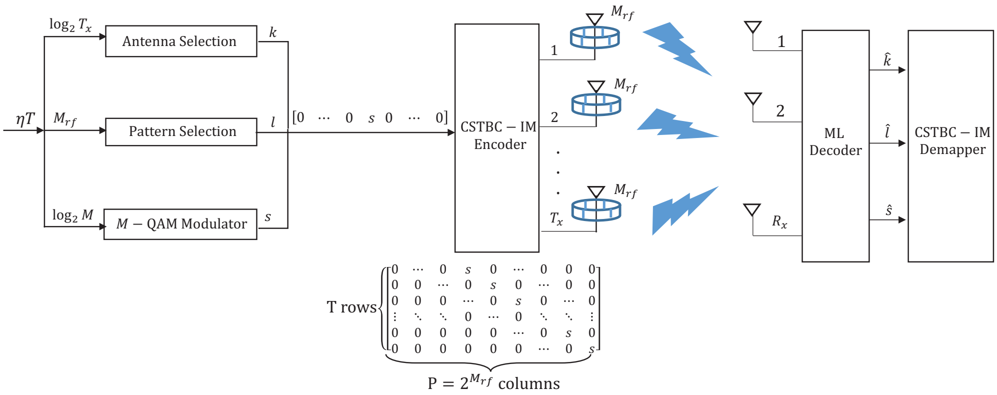

Fig. 1. Block Diagram of the CSTBC-SM scheme.

first time interval, where $l \in \{1,2,\ldots,P\}$, the overall transmission matrix $\mathbf{X} \in \mathbb{C}^{T\times P}$ of CSTBC-SIMO can be given as

$$\mathbf{X} = \begin{bmatrix} 0 & \ldots & 0 & \overbrace{s}^{l} & 0 & \ldots & 0 & 0 & 0 & 0 \\ 0 & 0 & \cdots & 0 & s & 0 & \cdots & 0 & 0 & 0 \\ \vdots & \ddots & \ddots & \ddots & \ddots & \ddots & \ddots & \ddots & \ddots & \vdots \\ 0 & 0 & \cdots & 0 & 0 & 0 & s & 0 & \cdots & 0 \end{bmatrix}. \quad (5)$$

The same signal transmission model as that of the CSTBC-SIMO scheme is also considered for the CSTBC-SSK scheme. However, unlike CSTBC-SIMO, instead of a modulated M-PSK/QAM signal, a cosine signal ($s = 1$) is transmitted over the effective channel state of each time interval.

B. CSTBC-SM and CSTBC-MIMO

In this subsection, to improve the spectral efficiency of the CSTBC-SIMO and CSTBC-SSK schemes, the proposed circular STBC concept is generalized for MIMO system configurations, and CSTBC-SM and CSTBC-MIMO transmission schemes are introduced.

The block diagram of the CSTBC-SM scheme is given in Fig. 1. In CSTBC-SM scheme, the incoming ηT bits determine the indices of both the active antenna and its effective channel state, as well as a modulated symbol from M-PSK/QAM constellations to be transmitted through this effective channel state. Therefore, the spectral efficiency of the CSTBC-SM scheme is given as

$$\eta_{SM} = \frac{M_{rf} + \log_2 T_x + \log_2 M}{T} \quad \text{[bpcu]}. \quad (6)$$

In the CSTBC-SM scheme, the incoming $\log_2 T_x$, M_{rf} and $\log_2 M$ bits determine the indices of an active antenna k, its corresponding channel state l and a M-PSK/QAM symbol s, respectively. Then, the transmission vector of the first transmission interval $\mathbf{x}_1 \in \mathbb{C}^{1\times PT_x}$ is constructed as:

$$\mathbf{x}_1 = [\underbrace{0\ 0\ \cdots\ 0}_{1}|\cdots|\underbrace{0\ \cdots\ 0\ \overbrace{s}^{l}\ 0\ \cdots\ 0}_{k}|\cdots|\underbrace{0\ 0\ \cdots\ 0}_{T_x}]. \quad (7)$$

where $k \in \{1,2,\cdots,T_x\}$ and $l \in \{1,2,\cdots,P\}$. Then, as to CSTBC-SIMO and CSTBC-SSK schemes, for the remaining $T-1$ time intervals, the structure of a circular matrix is followed and the overall transmission matrix $\mathbf{X} \in \mathbb{C}^{T\times PT_x}$ of the CSTBC-SM scheme is constructed as

$$\mathbf{X} = \left[\begin{array}{cccc|c|cccccccccc|c|cccc} 0 & 0 & \cdots & 0 & \cdots & 0 & \cdots & 0 & s & 0 & \cdots & 0 & 0 & 0 & 0 & \cdots & 0 & 0 & \cdots & 0 \\ 0 & 0 & \cdots & 0 & \cdots & 0 & 0 & \cdots & 0 & s & 0 & \cdots & 0 & 0 & 0 & \cdots & 0 & 0 & \cdots & 0 \\ \vdots & \vdots & \cdots & \vdots & \cdots & \vdots & \ddots & \ddots & \ddots & \ddots & \ddots & \ddots & \ddots & \ddots & \vdots & \cdots & \vdots & \vdots & \cdots & \vdots \\ 0 & 0 & \cdots & 0 & \cdots & 0 & 0 & \cdots & 0 & 0 & 0 & s & 0 & \cdots & 0 & \cdots & 0 & 0 & \cdots & 0 \end{array}\right]. \quad (8)$$

To further improve the spectral efficiency of the CSTBC-SM scheme, a novel CSTBC-MIMO transmission scheme is developed by adapting circular STBC concept to the MIMO-MBM scheme. In the CSTBC-MIMO transmission scheme, all available T_x transmit antennas are used in transmission through their effective channel states and T_x number of M-PSK/QAM modulated symbols are transmitted. Therefore, the spectral efficiency of the CSTBC-MIMO scheme is given as

$$\eta_{MIMO} = \frac{T_x(M_{rf} + \log_2 M)}{T} \quad \text{[bpcu]}. \quad (9)$$

In the CSTBC-MIMO transmission scheme, the first $T_x M_{rf}$ bits of the incoming ηT information bits determine an effective channel state l_i among P channel state realizations for each of T_x transmit antennas, where $l_i \in \{1,2,\ldots,P\}$. On the other hand, the remaining $T_x \log_2 M$ information bits determine s_i M-PSK/QAM symbols, for $i \in \{1,2,\ldots,T_x\}$, for the transmission over the selected channel states with the indices l_i. Then, the overall transmission matrix $\mathbf{X} \in \mathbb{C}^{T\times PT_x}$ of the CSTBC-MIMO scheme is given in (10), which is shown at the bottom of the next page.

C. Transmission Model

In the CSTBC-IM transmission schemes, $\mathbf{X} \in \mathbb{C}^{T\times PT_x}$ is transmitted over a channel created by different channel state realizations and represented by $\mathbf{H} \in \mathbb{C}^{PT_x\times R_x}$ while experiencing additive white Gaussian noise (AWGN) samples, denoted by $\mathbf{W} \in \mathbb{C}^{T \times R_x}$. The entries of the matrices $\mathbf{H}$ and $\mathbf{W}$ are modeled by independent and identically distributed (i.i.d.) complex Gaussian random variables with distributions of $\mathcal{C}(0,1)$ and $\mathcal{C}(0,\sigma^2)$, respectively. Then, the matrix of received signals $\mathbf{Y} \in \mathbb{C}^{T \times R_x}$ is obtained as

$$\mathbf{Y} = \mathbf{X}\mathbf{H} + \mathbf{W}. \tag{11}$$

For a general CSTBC-IM system, the received signals can also be given in the following equivalent model, for $\mathbf{y} = \mathrm{vec}(\mathbf{Y}) \in \mathbb{C}^{TR_x \times 1}$ and $\mathbf{w} = \mathrm{vec}(\mathbf{W}) \in \mathbb{C}^{TR_x \times 1}$, as

$$\mathbf{y} = \mathbf{H}_e \mathbf{s} + \mathbf{w} \tag{12}$$

where $\mathbf{s} = [s_1, s_2, \ldots, s_{T_x}]^{\mathrm{T}} \in \mathbb{C}^{T_x \times 1}$ and s_j is the modulated symbol transmitted over a particular channel state of the jth transmit antenna, for $j = \{1, 2, ..., T_x\}$, while $\mathbf{H}_e \in \mathbb{C}^{TR_x \times T_x}$ is the equivalent channel matrix containing the columns of $\mathbf{H}$ corresponding to the jth transmit antenna and $\mathrm{vec}(\cdot)$ is vectorization operator.

The receiver of the CSTBC-IM schemes is assumed to have perfect knowledge of the equivalent channel matrix $\mathbf{H}_e$ and consider a maximum likelihood (ML) detector to obtain an optimum BER performance by the following decision rule:

$$\hat{\mathbf{s}} = \arg\min_{\mathbf{s}} ||\mathbf{y} - \mathbf{H}_e \mathbf{s}||^2. \tag{13}$$

Then, the detected $\hat{\mathbf{s}}$ is demapped to determine the corresponding bits.

In CSTBC-IM schemes, both correlated and uncorrelated channel fading statistics are considered. For the case of correlated channels, a correlation is assumed among the channel states of each transmit antenna, where the correlation model is taken from a real multi-state reconfigurable antenna with $M_{rf} = 2$ and $P = 2^{M_{rf}} = 4$ channel states [20] and the correlation values among those channel states are represented by the following matrix $\mathbf{S} \in \mathbb{C}^{P \times P}$ [20]

$$\mathbf{S} = \begin{bmatrix} 1 & 0.0722 & 0.0593 & 0.0007 \\ 0.0772 & 1 & 0.0158 & 0.0522 \\ 0.0593 & 0.0158 & 1 & 0.0688 \\ 0.007 & 0.0522 & 0.0688 & 1 \end{bmatrix}. \tag{14}$$

For the case of correlated channel states, the correlated $\mathbf{H}$ matrix is constructed by an uncorrelated channel matrix $\tilde{\mathbf{H}} \in \mathbb{C}^{PT_x \times R_x}$ whose entries are i.i.d. complex Gaussian random variables with $\mathcal{C}(0,1)$ distribution, as follows:

$$\mathbf{H} = \mathbf{C}_t^{1/2} \tilde{\mathbf{H}} \mathbf{C}_r^{1/2} \tag{15}$$

where $\mathbf{C}_t$ and $\mathbf{C}_r$ are the transmit and received correlation matrices. Then, since no spatial correlation is assumed, $\mathbf{C}_t = \mathbf{I}_{T_x} \otimes \mathbf{S}$ and $\mathbf{C}_r = \mathbf{I}_{R_x}$, where $\mathbf{I}_n$ is an identity matrix with $n \times n$ dimensions and $\otimes$ shows the Kronecker product.

III. Performance Analysis

In this section, the pairwise error probability (PEP) of the CSTBC-IM transmission schemes is analytically derived and an upper bound expression for the ABEP of the CSTBC-IM schemes is obtained.

To determine the PEP of the proposed systems, first, an expression for conditional PEP is derived [21] for the transmission of $\mathbf{X}$ and its erroneous detection $\hat{\mathbf{X}}$, as follows

$$P_r\big(\mathbf{X} \to \hat{\mathbf{X}}|\mathbf{H}\big) = Q\left(\sqrt{\frac{||(\mathbf{X} - \hat{\mathbf{X}})\mathbf{H}||^2}{4\sigma^2}}\right). \tag{16}$$

Let $\mathbf{\Sigma} = ||\big(\mathbf{X} - \hat{\mathbf{X}}\big)\mathbf{H}||^2$ and $\mathbf{\Omega}$ be the following difference matrix

$$\mathbf{\Omega} = \big(\mathbf{X} - \hat{\mathbf{X}}\big)^{\mathrm{H}}\big(\mathbf{X} - \hat{\mathbf{X}}\big). \tag{17}$$

After some algebraic manipulations, $\mathbf{\Sigma}$ is given in quadratic form as

$$\begin{aligned} \mathbf{\Sigma} &= ||\big(\mathbf{X} - \hat{\mathbf{X}}\big)\mathbf{H}||^2 \\ &= \mathrm{vec}(\tilde{\mathbf{H}}^{\mathrm{H}})^{\mathrm{H}} (\mathbf{C}_s{}^{1/2})^{\mathrm{H}} (\mathbf{I}_{R_x} \otimes \mathbf{\Omega}) \mathbf{C}_s{}^{1/2} \mathrm{vec}(\tilde{\mathbf{H}}^{\mathrm{H}}) \end{aligned} \tag{18}$$

where $\mathbf{C}_s = \mathbf{C}_t \otimes \mathbf{C}_r$. Then, considering the following alternative Q-function expression

$$Q(x) = \frac{1}{\pi}\int_0^{\pi/2} \exp\left(\frac{-x^2}{2\sin^2\phi}\right) d\phi \tag{19}$$

and substituting (18) into (19), (16) can be rewritten as

$$\begin{aligned} &P_r\left(\mathbf{X} \to \hat{\mathbf{X}}|\mathbf{H}\right) \\ &= \frac{1}{\pi}\int_0^{\pi/2} \exp\left(-\gamma \frac{\mathrm{vec}(\tilde{\mathbf{H}}^{\mathrm{H}})^{\mathrm{H}} \mathbf{\Delta}\, \mathrm{vec}(\tilde{\mathbf{H}}^{\mathrm{H}})}{4\sin^2\phi}\right) d\phi \end{aligned} \tag{20}$$

where $\gamma = 1/2\sigma^2$ and $\mathbf{\Delta} = (\mathbf{C}_s{}^{1/2})^{\mathrm{H}}(\mathbf{I}_{R_x} \otimes \mathbf{\Omega})\mathbf{C}_s{}^{1/2}$. Then, averaging (20) over $\mathbf{H}$ and considering a moment generating function (MGF) approach [22], the PEP expression is obtained in (21), where $\mathbf{z} = \mathrm{vec}(\tilde{\mathbf{H}}^{\mathrm{H}})$, $\bar{\mathbf{z}}$ is the mean vector and $\mathbf{K}_{\mathbf{z}} = E\left\{\mathbf{z}^{\mathrm{H}}\mathbf{z}\right\} - \bar{\mathbf{z}}^{\mathrm{H}}\bar{\mathbf{z}}$ is the covariance matrix. Then, since $\bar{\mathbf{z}} = 0$ and $\mathbf{K}_{\mathbf{z}} = \mathbf{I}_{PT_xR_x}$ for the Rayleigh fading channel matrix $\tilde{\mathbf{H}}$, the PEP of the CSTBC-IM schemes simplifies to

$$P_r\big(\mathbf{X} \to \hat{\mathbf{X}}\big) = \frac{1}{\pi}\int_0^{\pi/2} \det\left[\mathbf{I}_{PT_xR_x} + \gamma \frac{\mathbf{\Delta}}{4\sin^2\phi}\right]^{-1} d\phi. \tag{22}$$

$$\mathbf{X} = \left[\begin{array}{cccccccccc|cccccccccc|c|cccccccccc} 0 & \cdots & 0 & s_1 & 0 & \cdots & 0 & 0 & 0 & 0 & 0 & \cdots & 0 & s_2 & 0 & \cdots & 0 & 0 & 0 & 0 & \cdots & 0 & \cdots & 0 & s_{T_x} & 0 & \cdots & 0 & 0 & 0 & 0 \\ 0 & 0 & \cdots & 0 & s_1 & 0 & \cdots & 0 & 0 & 0 & 0 & 0 & \cdots & 0 & s_2 & 0 & \cdots & 0 & 0 & 0 & \cdots & 0 & 0 & \cdots & 0 & s_{T_x} & 0 & \cdots & 0 & 0 & 0 \\ \vdots & \ddots & \ddots & \ddots & \ddots & \ddots & \ddots & \ddots & \ddots & \vdots & \vdots & \ddots & \ddots & \ddots & \ddots & \ddots & \ddots & \ddots & \ddots & \vdots & \cdots & \vdots & \ddots & \ddots & \ddots & \ddots & \ddots & \ddots & \ddots & \ddots & \vdots \\ 0 & 0 & \cdots & 0 & 0 & 0 & s_1 & 0 & \cdots & 0 & 0 & 0 & \cdots & 0 & 0 & 0 & s_2 & 0 & \cdots & 0 & \cdots & 0 & 0 & \cdots & 0 & 0 & 0 & s_{T_x} & 0 & \cdots & 0 \end{array}\right] \tag{10}$$

Moreover, to derive a closed form expression, an upper bound is obtained in terms of the non-zero eigenvalues λ_m of the difference matrix $\mathbf{\Omega}$ (17) by letting $\phi = \frac{\pi}{2}$, as follows

$$P_r\big(\mathbf{X} \rightarrow \hat{\mathbf{X}}\big) \leq \frac{1}{2}\left[\prod_{m=1}^{T}\left(\frac{1}{1+\gamma\frac{\lambda_m}{4}}\right)^{N_r}\right]. \quad (23)$$

Then, using the well-known union bound approach [21], ABEP is obtained as:

$$P_b \leq \frac{1}{2^{\kappa}}\sum_{\mathbf{X}}\left[\frac{1}{\kappa}\sum_{\hat{\mathbf{X}}} Pr\big(\mathbf{X} \rightarrow \hat{\mathbf{X}}\big)\beta\big(\mathbf{X}, \hat{\mathbf{X}}\big)\right] \quad (24)$$

where $\beta\big(\mathbf{X}, \hat{\mathbf{X}}\big)$ is the number of bit errors for each $\big(\mathbf{X} \rightarrow \hat{\mathbf{X}}\big)$ error event and $\kappa = \eta T$ is the total number of incoming data bits.

IV. Simulation Results

In this section, the BER performance of CSTBC-IM schemes are investigated via comprehensive theoretical and Monte Carlo simulations to reveal the flexibility of the proposed schemes, which attain both high and low spectral efficiency values while achieving a Tth order transmit diversity gain. All simulations are sketched as a function of received energy per bit to noise ratio (E_b/N_0), where $N_0 = 2\sigma^2$, for $R_x = 4$.

In Fig. 2, theoretical and computer simulation results of the CSTBC-SSK scheme achieving a Tth order transmit diversity gain are shown for low spectral efficiency values, where T ranges from 2 to 32. These results show that the computer simulation curves are in perfect agreement with the theoretical curves at high E_b/N_0 values. In addition, the effect of increasing transmit diversity on the BER performance is clearly observed, where the BER improves as T increases.

The BER performance of CSTBC-IM schemes that achieve various spectral efficiency values are demostrated in Fig. 3. It can be deduced from Figs. 2 and 3 that the proposed CSTBC-IM schemes enable a Tth order transmit diversity gain at both low and high spectral efficiency values.

In Fig. 4, for $T = 2$, the BER performance of the proposed CSTBC-IM schemes over correlated and uncorrelated channel statistics is investigated. For the correlated channel conditions, the correlation is assumed only among the channel state realizations of each transmit antenna, where the correlation matrix $\mathbf{S}$ given in (14) of a real multi-state transmit antenna with $M_{rf} = 2$ and $P = 2^{M_{rf}} = 4$, is considered. For the CSTBC-SIMO and CSTBC-SSK schemes, which respectively attain $\eta = 1$ and 2 bpcu spectral efficiency values, the BER results under the correlated channel conditions are nearly 2 dB behind the uncorrelated case. However, when the same channel state correlation is assumed without any spatial correlation, the BER performance of CTBC-SM, for $T_x = 4$, $M_{rf} = 2$ and QPSK, is almost the same as the uncorrelated case.

In Fig. 5, the BER performance of CSTBC-MIMO scheme is compared to that of the-state-of-the-art transmission schemes achieving a second order transmit diversity gain at $\eta = 6$ bpcu. The results show that the BER performance of the CSTBC-MIMO scheme for $T_x = 2$, $M_{rf} = 4$ and QPSK is far beyond the traditional STBC-based IM schemes [15]–[18] while it achieves a nearly 0.5 dB E_b/N_0 gain over the recent STCM scheme [12].

V. Conclusion

In this paper, the family CSTBC-IM schemes, which achieve various orders of transmit diversity gains with a single RF chain, has been proposed for beyond 5G ultra reliable communication applications. The error performance of CSTBC-IM schemes has been theoretically analyzed and an upper bound expression for ABEP has been derived. Through extensive Monte Carlo simulations, the flexibility of the proposed systems to attain higher spectral efficiency values while providing various transmit diversity gains have been shown, which can make the CSTBC-IM schemes as a potential enabler for beyond 5G ultra reliable communication applications.

References

[1] E. De Carvalho, E. Bjornson, J. H. Sorensen, P. Popovski, and E. G. Larsson, "Random access protocols for massive MIMO," *IEEE Commun. Mag.*, vol. 55, no. 5, pp. 216–222, 2017.

[2] J. J. Nielsen, R. Liu, and P. Popovski, "Ultra-reliable low latency communication using interface diversity," *IEEE Trans. Commun.*, vol. 66, no. 3, pp. 1322–1334, 2018.

[3] M. Bennis, M. Debbah, and H. V. Poor, "Ultra-reliable and low-latency wireless communication: Tail, risk and scale," *arXiv preprint arXiv:1801.01270*, Aug. 2018.

[4] E. Basar, M. Wen, R. Mesleh, M. Di Renzo, Y. Xiao, and H. Haas, "Index modulation techniques for next-generation wireless networks," *IEEE Access*, vol. 5, pp. 16 693–16 746, 2017.

[5] R. Mesleh, H. Haas, S. Sinanovic, C. W. Ahn, and S. Yun, "Spatial modulation," *IEEE Trans. Veh. Technol.*, vol. 57, no. 4, pp. 22–28, July 2008.

[6] Y. Naresh and A. Chockalingam, "On media-based modulation using RF mirrors," *IEEE Trans. Veh. Technol.*, vol. 66, no. 6, pp. 4967–4983, June 2017.

[7] M. Yüzgeçcioğlu and E. Jorswieck, "Performance of media-based modulation in multi-user networks," in *Proc. the Int. Symp. Wireless Commun. Systems*, Aug. 2017.

[8] B. Shamasundar, S. Jacob, L. N. Theagarajan, and A. Chockalingam, "Media-based modulation for the uplink in massive MIMO systems," *IEEE Trans. Veh. Technol.*, vol. 67, no. 9, pp. 8169 – 8183, Sept. 2018.

$$P_r\left(\mathbf{X} \rightarrow \hat{\mathbf{X}}\right) = \frac{1}{\pi}\int_0^{\pi/2} \frac{\exp\left(-\bar{\mathbf{z}}^{\mathrm{H}}\frac{\gamma}{4\sin^2\phi}\mathbf{\Delta}\left(\mathbf{I}_{PT_xR_x} + \frac{\gamma}{4\sin^2\phi}\mathbf{K_z}\mathbf{\Delta}\right)^{-1}\bar{\mathbf{z}}\right)}{\det\left(\mathbf{I}_{PT_xR_x} + \frac{\gamma}{4\sin^2\phi}\mathbf{K_z}\mathbf{\Delta}\right)} d\phi. \quad (21)$$

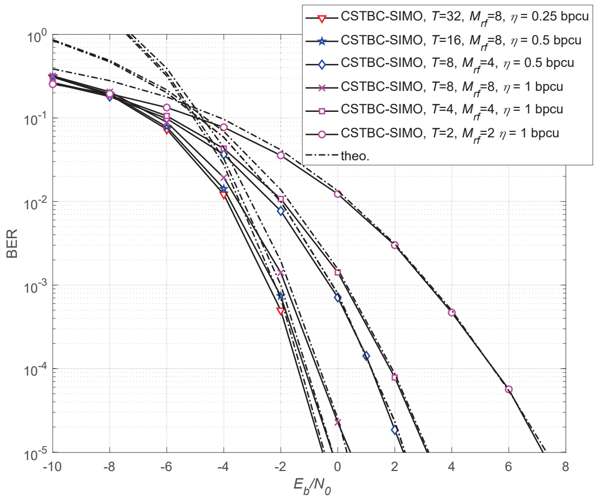

Fig. 2. The theoretical and Monte Carlo simulation results of CSTBC-SSK scheme at low spectral efficiency values for $R_x = 4$.

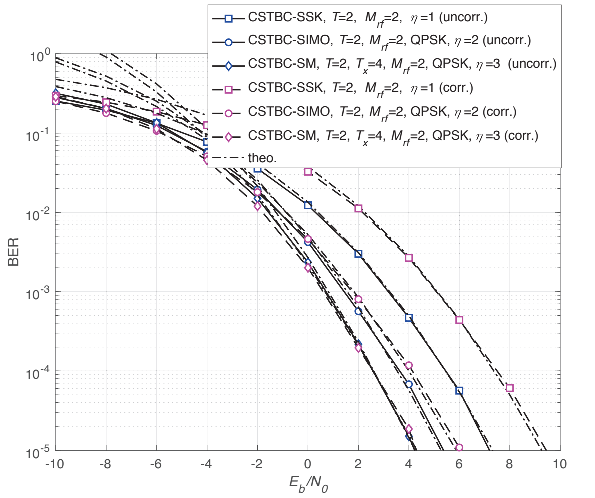

Fig. 4. The BER performance of the CSTBC-IM schemes with $M_{rf} = 2$ for correlated [20] and uncorrelated channel statistics and $R_x = 4$.

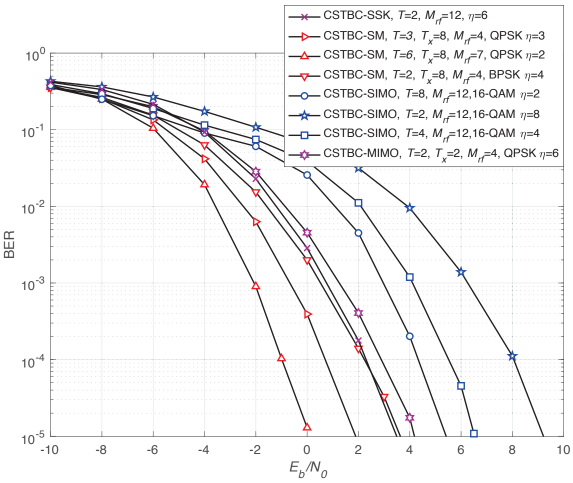

Fig. 3. The BER performance of the CSTBC-IM schemes for various spectral efficiency values and $R_x = 4$.

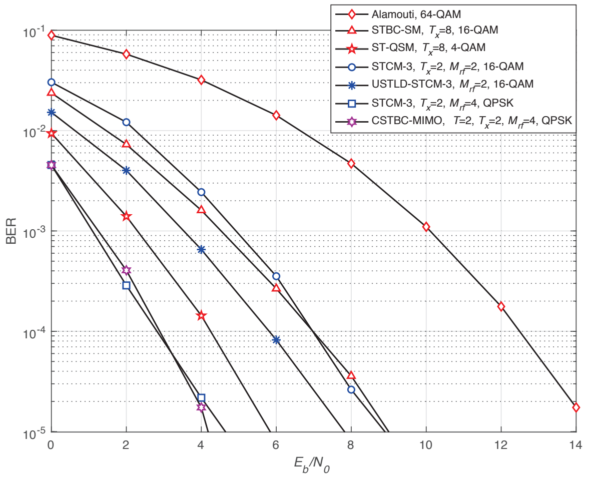

Fig. 5. The BER performance of CSTBC-MIMO, STCM [12], STBC-SM [15], USTLD-STCM [16], ST-QSM [18] and Alamouti's STBC [17] schemes for $\eta = 6$ bpcu and $R_x = 4$.

[9] B. Shamasundar and A. Chockalingam, "Multiuser media-based modulation for massive MIMO systems," in *Proc. Signal Process. Advances in Wireless Commun. (SPAWC), IEEE 18th Int. Workshop*, pp. 1–5.

[10] I. Yildirim, E. Basar, and G. Kurt, "Media-based modulation for secrecy communications," *IET Electron. Lett.*, vol. 54, pp. 789–791, June 2018.

[11] L. Zhang and M. Zhao, "Secrecy enhancement for media-based modulation via probabilistic optimization," *IEEE Commun. Lett.*, Dec. 2018.

[12] E. Basar and I. Altunbas, "Space-time channel modulation," *IEEE Trans. Veh. Technol.*, vol. 66, no. 8, pp. 7609–7614, 2017.

[13] E. Basar, "Media-based modulation for future wireless systems: A tutorial," *IEEE Wireless Commun.*, (to appear) Mar. 2019.

[14] Z. Yigit and E. Basar, "Space-time media-based modulation," *IEEE Trans. Signal Process.*, (to appear) Mar. 2019.

[15] E. Basar, U. Aygolu, E. Panayirci, and H. V. Poor, "Space-time block coded spatial modulation," *IEEE Trans. Commun.*, vol. 59, no. 3, pp. 823–832, Mar. 2011.

[16] N. Pillay and H. Xu, "Uncoded space-time labeling diversityapplication of media-based modulation with RF mirrors," *IEEE Commun. Lett.*, vol. 22, no. 2, pp. 272–275, Feb. 2018.

[17] S. M. Alamouti, "A simple transmit diversity technique for wireless communications," *IEEE J. Sel. Areas Commun.*, vol. 16, no. 8, pp. 1451–1458, Oct. 1998.

[18] Z. Yigit and E. Basar, "Space-time quadrature spatial modulation," in *Proc. IEEE International Black Sea Conf. Commun. Netw. (BlackSeaCom)*, 2017.

[19] H. Jafarkhani, *Space-time coding: theory and practice*. Cambridge University Press, 2005.

[20] D.-T. Phan-Huy, Y. Kokar, K. Rachedi, P. Pajusco, A. Mokh, T. Magounaki, R. Masood, C. Buey, P. Ratajczak, N. Malhouroux-Gaffet *et al.*, "Single-carrier spatial modulation for the Internet of Things: Design and performance evaluation by using real compact and reconfigurable antennas," *IEEE Access*, vol. 7, pp. 18 978–18 993, Jan. 2019.

[21] M. K. Simon and M.-S. Alouini, *Digital communication over fading channels*. John Wiley & Sons, vol. 95, 2005.

[22] G. L. Turin, "The characteristic function of Hermitian quadratic forms in complex normal variables," *Biometrika*, vol. 47, no. 1/2, pp. 199–201, June 1960.